The α7 nicotinic receptor silent agonist R-47 prevents and reverses paclitaxel-induced peripheral neuropathy in mice without tolerance or altering nicotine reward and withdrawal

Wisam Toma[1], **S. Lauren Kyte**[2], **Deniz Bagdas**[3], **Asti Jackson**[3], **Julie A. Meade**[1], **Faria Rahman**[1], **Zhi-Jian Chen**[4], **Egidio Del Fabbro**[5,6], **Lucas Cantwell**[7], **Abhijit Kulkarni**[7], **Ganesh A. Thakur**[7], **Roger L. Papke**[8], **John W. Bigbee**[9], **David A. Gewirtz**[1], **M. I. Damaj**[1,6]

[1]Department of Pharmacology and Toxicology, Virginia Commonwealth University, Richmond, VA;

[2]Center for Veterinary Medicine, U.S. Food and Drug Administration, Rockville, MD;

[3]Department of Psychiatry, Yale University School of Medicine, Yale Tobacco Center of Regulatory Science, New Haven, CT;

[4]Department of Neurology, Virginia Commonwealth University, Richmond, VA;

[5]Department of Internal Medicine, Virginia Commonwealth University, Richmond, VA;

[6]Translational Research Initiative for Pain and Neuropathy, Virginia Commonwealth University, Richmond, VA;

[7]Department of Pharmaceutical Sciences, Northeastern University, Boston, MA;

[8]Department of Pharmacology and Therapeutics, College of Medicine, University of Florida, Gainesville, FL.

[9]Department of Anatomy and Neurobiology, School of Medicine, Virginia Commonwealth University, Richmond, VA;

Abstract

Various antitumor drugs, including paclitaxel, frequently cause chemotherapy-induced peripheral neuropathy (CIPN) that can be sustained even after therapy has been completed. The current work was designed to evaluate R-47, an α7 nAChR silent agonist, in our mouse model of CIPN. R-47 was administered to male C57BL/6J mice prior to and during paclitaxel treatment. Additionally, we tested if R-47 would alter nicotine's reward and withdrawal effects. The H460 and A549 non-small cell lung cancer (NSCLC) cell lines were exposed to R-47 for 24–72 hours, and tumor-bearing NSG mice received R-47 prior to and during paclitaxel treatment. R-47 prevents and

Corresponding author: Wisam Toma, Ph.D. Department of Pharmacology and Toxicology, School of Medicine, Virginia Commonwealth University; Hermes A. Kontos Medical Sciences Building, 1217 E Marshall Street, Room# 334, Richmond, VA, 23298. Phone: 804-828-2956; Fax: 804-827-1548; tomawb@vcu.edu.

reverses paclitaxel-induced mechanical hypersensitivity in mice in an α7 nAChR-dependent manner. No tolerance develops following repeated administration of R-47, and the drug lacks intrinsic rewarding effects. Additionally, R-47 neither changes the rewarding effect of nicotine in the Conditioned Place Preference test nor enhances mecamylamine-precipitated withdrawal. Furthermore, R-47 prevents paclitaxel-mediated loss of intraepidermal nerve fibers and morphological alterations of microglia in the spinal cord. Moreover, R-47 does not increase NSCLC cell viability, colony formation, or proliferation, and does not interfere with paclitaxel-induced growth arrest, DNA fragmentation, or apoptosis. Most importantly, R-47 does not increase the growth of A549 tumors or interfere with the antitumor activity of paclitaxel in tumor-bearing mice. These studies suggest that R-47 could be a viable and efficacious approach for the prevention and treatment of CIPN that would not interfere with the antitumor activity of paclitaxel or promote lung tumor growth.

Keywords

α7 nAChR; Paclitaxel; Neuropathy; Cancer; Mice; Withdrawal

Introduction

The utilization of cancer chemotherapeutic drugs, specifically paclitaxel, oxaliplatin, vincristine, and bortezomib, is associated with the painful side effects of chemotherapy-induced peripheral neuropathy (CIPN). The peripheral neuropathy induced by paclitaxel, a taxane used to treat breast, ovarian, and non-small cell lung cancers, involves sensory symptoms including burning pain, numbness, tingling, and both cold and mechanical allodynia (Hagiwara and Sunada, 2004). These symptoms can persist for several years after the cessation of chemotherapy in approximately 30% of patients who receive the drug (Ewertz et al., 2015). Unfortunately, there is no effective treatment to prevent or alleviate this peripheral neuropathy.

Recent studies from our lab and others demonstrated that nicotine prevented and reversed important aspects of CIPN in rodent models (Di Cesare Mannelli et al., 2013; Kyte et al., 2018). Nicotine acts on multiple nicotinic acetylcholine receptors (nAChRs) subtypes, such as α4β2*, α3β4* and α7 subtypes. However, tolerance and undesirable psychoactive (α4β2*-mediated dependence) and gastrointestinal (α3β4*-mediated) side effects are associated with nicotine's antinociceptive effects. A growing body of evidence suggests that the homomeric α7 nAChR subtype is a viable target for the treatment of inflammatory, acute, and chronic pain, as well as neurodegenerative diseases (Bencherif et al., 2011). The α7 nAChR subtype is expressed throughout the pain transmission pathway on neuronal cells located in the brain, spinal cord, dorsal root ganglia (DRG) (Cordero-Erausquin et al., 2004), and on non-neuronal cells, including immune cells, such as macrophages (Tracey, 2002). In addition, we recently showed that targeting nAChRs with nicotine, a full agonist, reverses and prevents the CIPN induced by paclitaxel, at least in part via an α7 nAChR-dependent mechanism (Kyte et al., 2018).

Traditional α7 nAChR agonists and allosteric modulators (type I PAMs, type II PAMs, and Ago-PAMs) open ion channels to elicit their effects (Bagdas et al., 2017). A novel series of low efficacy (<2%) "silent agonists" bind selectively to the α7 nAChR and induce conformational changes in the receptor; however, this conformation does not cause the channel to open or induce a current, but instead stabilizes a PAM-sensitive desensitized state, which produces a pharmacological effect (Briggs et al., 2009; Papke et al., 2018). For example, the selective α7 silent agonist NS6740 reverses sensory and affective aspects of chronic pain in mouse models (Papke et al., 2015). Further, the silent agonist R-47, which has high α7 affinity and selectivity, with favorable pharmacokinetic properties, prevents disease onset and reduces inflammation in a collagen-induced arthritis mouse model (van Maanen et al., 2015).

In this work, we investigated the potential of targeting the α7 nAChR with the silent agonist R-47 in our model of paclitaxel-induced CIPN (Toma et al., 2017). We studied the impact of R-47 on paclitaxel-induced inflammatory responses in spinal microglia (McMahon et al., 2015), which are also involved in the pathology of nerve injury and neuropathic pain (for review, see (Chen et al., 2018)). Additionally, we probed the ability of R-47 to induce spontaneous pain relief in paclitaxel-treated mice using the conditioned place preference (CPP) test. We also evaluated whether R-47 would behave similarly to nicotine and elicit reward in the conditioned place preference (CPP) test or precipitate a withdrawal syndrome in mice treated chronically with nicotine (Jackson et al., 2015; Kallupi and George, 2017). Further, we assessed whether R-47 interacts with non-small cell lung cancer (NSCLC) progression and chemosensitivity both *in vitro* and *in vivo*, which is crucial if the compound will be used as a preventative and/or therapeutic treatment for CIPN in cancer patients.

Materials and Methods

Drugs.

Paclitaxel was purchased from Tocris (1097, Bristol, United Kingdom) and dissolved in a mixture of 1:1:18 [1 volume ethanol/1 volume Emulphor-620 (Rhone-Poulenc, Inc., Princeton, NJ)/18 volumes distilled water]. Paclitaxel was administered at a dose of 8 mg/kg i.p for one cycle to induce CIPN intraperitoneally (i.p.) every other day for a total of four injections to induce neuropathy, as previously described by (Toma et al., 2017). All the reversal and mechanistic studies were conducted at day 7–14 after initial paclitaxel injection unless otherwise noticed. The silent agonist R-47, (R)-N-(4-Methoxyphenyl)-2-((pyridin-3-yloxy)methyl)piperazine-1-carboxamide Dihydrochloride, was synthesized by following the experimental procedure reported by (Clark et al., 2014). R-47 was dissolved in distilled water (D.W).

For acute administration, R-47 was injected per os (p.o.) at doses of 1, 5, 10 mg/kg. The range of doses used in this study were chosen based on the previous studies that showed R-47 was effective to reduce the inflammatory response in different inflammatory pain assays (Clark et al., 2014; van Maanen et al., 2015). For chronic administration (prevention study), R-47 was injected p.o. at a dose of 10 mg/kg twice daily (8 hours apart) 3 days prior and during paclitaxel injection cycle. Von Frey test was performed 24 hours after daily R-47 treatment. For the tolerance study, we chose the dose that fully reversed and prevented

CIPN. For that, R-47 was administered p.o. at a dose of 10 mg/kg twice daily (8 hours apart) for 4 days to paclitaxel-treated group of mice. Methyllycaconitine (MLA) was purchased from RBI (Natick, MA, USA), dissolved in saline and was administered at a dose of 10 mg/kg subcutaneously (s.c.) 10 minutes before administration of R-47 (Freitas et al., 2013).

(−)-Nicotine hydrogen tartrate [(−)-1-methyl-2-(3- pyridyl) pyrrolidine (+)-bitartrate] and mecamylamine HCl (non-selective nAChR antagonist) were purchased from Sigma-Aldrich Inc. (St. Louis, MO, USA). Drugs were dissolved in physiological saline and administered subcutaneously (s.c.). Freshly prepared solutions were given to mice at 10 ml/kg. All doses are expressed as the free base of the drug. For the tumor-bearing animal study, paclitaxel was purchased from the VCU Health Pharmacy (NDC# 0703-4768-01, TEVA Pharmaceuticals, North Wales, PA) and diluted in a mixture of 1:1:18 [1 volume ethanol/1 volume Emulphor-620 (Rhone-Poulenc, Inc., Princeton, NJ)/18 volumes distilled water]. Paclitaxel injections of 10 mg/kg were administered intraperitoneally (i.p.) every day for a total of four injections; the injection site was swabbed with 70% ethanol prior to injection. R-47 was administered chronically at a dose of 10 mg/kg twice daily (one dose in the morning and one dose in the afternoon) via oral gavage for three days, then once daily in the morning followed by a 3-hour rest before a paclitaxel/vehicle injection for 4 days. These paclitaxel and R-47 regimens were chosen based on previous unpublished studies that demonstrated which dose, duration of exposure, and route of administration for each drug effectively arrested tumor growth or prevented paclitaxel-induced peripheral neuropathy, respectively, but were not toxic to the animal. All i.p., s.c., and p.o. injections were given in a volume of 10 ml/kg body weight.

For the cell culture studies, paclitaxel was dissolved in DMSO, diluted with sterile PBS, and added to the medium in order to obtain the desired concentration. Cells were not exposed to greater than 0.1% DMSO in any experiment. R-47 was dissolved in sterile PBS. All experiments involving these light-sensitive drugs were performed in the dark.

Animals.

Adult male C57BL/6J mice (8 weeks at the beginning of experiments, 20–30 g) were purchased from The Jackson Laboratory (Bar Harbor, ME). Adult ICR male mice (8 weeks at the beginning of experiments, 25–30 g) were purchased from Envigo Laboratories (Indianapolis, IN). Adult male NOD scid gamma (NSG) mice (8 weeks at the beginning of experiments, 20–30 g) were received as a gift from Dr. J. Chuck Harrell at Virginia Commonwealth University. Mice were housed in an AAALAC-accredited facility in groups of four. Food and water were available ad libitum. The mice in each cage were randomly allocated to different treatment groups. All behavioral testing on animals was performed in a blinded manner; behavioral assays were conducted by an experimenter blinded to the treatment groups. Experiments were performed during the light cycle (7:00 am to 7:00 pm) and were approved by the Institutional Animal Care and Use Committee of Virginia Commonwealth University and followed the National Institutes of Health Guidelines for the Care and Use of Laboratory Animals. Animals were euthanized via CO_2 asphyxiation, followed by cervical dislocation. Any subjects that showed behavioral disturbances unrelated to chemotherapy-induced pain were excluded from further behavioral testing.

Mechanical Sensitivity Evaluation (von Frey test).

Mechanical hypersensitivity thresholds were determined using von Frey filaments according to the method suggested by (Chaplan et al., 1994) and as described in our previous report (Bagdas et al., 2015). The mechanical threshold is expressed as log10 (10 £ force in [mg]).

Locomotor Activity Test.

The test was performed as previously described by Bagdas et al (Bagdas et al., 2015) Briefly, mice were placed into individual Omnitech (Columbus, OH) photocell activity cages (28×16.5 cm) containing two banks of eight cells each. Interruptions of the photocell beams, which assess walking and rearing, were then recorded for the next 30 min. Data are expressed as the number of photocell interruptions. R-47 (10 mg/kg, p.o.) or distilled water was administered to paclitaxel or vehicle groups of mice 180 min before testing in locomotor boxes.

Rotarod Test.

The rotarod test (IITC Inc. Life Science, Woodland Hills, CA, USA) was used to assess motor coordination as previously described by Freitas et al (Freitas et al., 2013). Percent impairment was calculated as follows: % impairment = [(180 _test time)/180] * 100. R-47 (10 mg/kg, p.o.) or distilled water was administered to paclitaxel or vehicle groups of mice 180 min before testing.

Immunohistochemistry and Characterization of Morphological Changes of Microglial Cells.

For the prevention study, the hind paw plantar skin was collected from the following groups of mice: vehicle-vehicle, vehicle-R-47 (10 mg/kg/), paclitaxel (8 mg/kg)-vehicle, and paclitaxel (8 mg/kg)-R-47 (10 mg/kg). The staining procedure was performed as previously described (Toma et al., 2017) with slight modifications. The glabrous skin of the hind paw was excised, placed in freshly prepared 4% paraformaldehyde in 0.1 M PBS (pH 7.4), and stored overnight at 4°C in the same fixative. Tissues were transferred to 30% sucrose and stored overnight in the refrigerator. Samples were embedded in optimum cutting temperature (O.C.T) compound (cat# 23-730-571, Fisher Scientific, USA) and twenty-micron cryostat sections were collected on glass slides for. Sections were immersed in ice-cold acetone for 20 minutes, washed with PBS, and incubated at room temperature for 30 min in blocking solution (5% normal goat serum and 0.3% Triton X-100 in PBS). Sections were incubated with a 1:1000 dilution of the primary antibody, PGP9.5 (Fitzgerald - cat# 70R-30722, MA, USA) overnight at 4°C in a humidity chamber. Following PBS washes, sections were incubated for 90 min at room temperature with a 1:250 dilution of goat anti-rabbit IgG (H +L) secondary antibody conjugated with Alexa Fluor® 594 (Life Technologies - cat# A11037, OR, USA). Sections were mounted in Vectashield (Vector Laboratories, Burlingame, CA, USA) and examined using a Zeiss Axio Imager A1 – Fluorescence microscope (Carl Zeiss, AG, Germany). Sections were examined in a blinded fashion under 63x magnification. Main fibers were counted in real time by dynamically focusing and following nerve fibers once they crossed the junction of the basement membrane. Density of fibers is expressed as fibers/mm.

Spinal cords from the same groups of mice mentioned previously were collected by hydraulic extrusion (Richner et al., 2017). The L4–L6 lumbar region of the spinal cord was collected and transferred to a freshly prepared 4% paraformaldehyde in 0.1 M PBS (pH 7.4) and stored overnight at 4°C in the same fixative. Twenty-micron cryostat sections were collected on glass slides and immunostained for microglia according to the same protocol used for the IENFs using the rabbit polyclonal anti-ionized calcium binding adaptor molecule 1 (Iba1) antibody at a dilution of 1:1000 (Wako chemicals, cat# 019–19741, Richmond, VA, USA). Characterization of microglial cell morphology was based on a previous study by (Zheng et al., 2011) with modifications. Microglial cells were binned into three main stages; Stage I: cells with long, thin, and highly ramified processes, Stage II: cells with shorter, thickened processes with less branching, and Stage III: cells displaying more hypertrophic changes such as short, thickened processes and enlargement of the cell body.

Regions of the dorsal horn including laminae 1–5 were examined using a Zeiss AxioImager Z2 equipped with a motorized XY stage, microcator Microbrightfield Neurolucida and Stereo Investigator image analysis software (MBF Bioscience, VT, USA). Microglia were identified and scored as indicated above using a 63x oil immersion objective in a blinded fashion. Images were acquired as z-stacks and results are reported as number of microglial cells per section.

Conditioned Place Preference (CPP) Test.

To determine if R-47 could alleviate spontaneous, ongoing pain in paclitaxel-treated mice but not in vehicle-treated mice, an unbiased CPP paradigm was conducted as previously described by (Grabus et al., 2012) with modifications. Briefly, the CPP test boxes (20×20×20 cm each; ENV3013; Med Associates, St Albans, VT, USA) consist of two main chambers equipped with two different colors and textures (white mesh or black rod), and a neutral gray middle chamber with a smooth PVC floor. Mice were handled for three weeks prior to conditioning. Mice were placed into the gray chamber to acclimate for 5 min, then allowed to freely move between all CPP boxes for 15 min. This is considered the preconditioning baseline measurement. After that, mice were assigned randomly into four groups; one paclitaxel group received distilled water and the other paclitaxel group received R-47 at a dose of 10 mg/kg p.o.; a similar approach was applied to the vehicle-treated groups. Mice received R-47 or its vehicle (distilled water) on alternative days. i.e. the group that received R-47 on one day (one injection per day) should receive distilled water on the next. A total 8 conditioning days was applied. R-47 or vehicle was administered two hours prior to placing the mice into the corresponding CPP boxes for 30 min. On the test day, mice were placed into the gray CPP box and allowed to freely move between the boxes for 15 min in a drug-free state. The preference score was calculated by determining the difference between time spent in the drug-paired side on the test day minus the time in the drug-paired side on the baseline day. An alternative experimental design was implemented to test wither R-47 would affect nicotine's rewarding properties (Jackson et al., 2017). On day 1, animals were confined to the middle chamber for a 5-min habituation and then allowed to freely move between all three chambers for 15 min. Time spent in each chamber was recorded, and these data were used to populate groups of approximately equal bias in baseline chamber preference. Twenty-minute conditioning sessions occurred twice a day (days 2–4). During

conditioning sessions, mice were confined to one of the larger chambers. The control groups received saline in one large chamber in the morning and saline in the other large chamber in the afternoon. The drug group received nicotine in one large chamber and saline in the other large chamber. On each of the conditioning days, mice were pretreated with R-47 (at 1 or 10 mg/kg, p.o) or vehicle 120 min prior to nicotine. Treatments were counterbalanced to ensure some mice received the unconditioned stimulus in the morning and others received it in the afternoon. The drug-paired chamber was randomized across groups. Sessions were 4 hours apart and were conducted by the same investigator. On test day (day 5), mice could access all chambers for 15 min in a drug free state. The preference score was calculated by determining the difference between time spent in the drug paired side on the test day versus the time in drug paired side on the baseline day.

Nicotine Precipitated Withdrawal Studies.

Mice were infused with 24 mg/kg/day nicotine or saline for 14 days using s.c. osmotic minipumps (model 2000; Alzet Corporation, Cupertino, CA) implanted under isoflurane anesthesia (Jackson et al., 2008). Nicotine concentration was adjusted according to animal weight and mini pump flow rate. On the morning of day 15, mice were pretreated with vehicle, R-47 (10 mg/kg, p.o; 120 min prior) before challenge with the non-selective nAChR antagonist, mecamylamine (2 mg/kg, s.c.) to precipitate withdrawal. Anxiety-like behaviors, somatic signs and hyperalgesia nicotine withdrawal signs were evaluated 10 min later as described in Jackson et al (Jackson et al., 2008). Mice were first evaluated for 5 min in the Light-dark box (LBD) Test. The number of entries into the light compartment, the number of transitions and the total time spent in the light compartment were recorded for 5 min by a video monitoring technique and ANY-MAZE software (Stoelting Co., Wood Dale, IL). Animals were then observed for 30 min time for somatic signs measured as paw and body tremors, head shakes, backing, jumps, curls, and ptosis. Mice were placed in clear activity cages without bedding for the observation period. The total number of somatic signs was tallied for each mouse and the average number of somatic signs during the observation period was plotted for each test group. Hyperalgesia was finally evaluated using the hot plate test immediately following the somatic sign observation period. Mice were placed into a 10-cm wide glass cylinder on a hot plate (Thermojust Apparatus, Richmond, VA) maintained at 52°C. The latency to reaction time (jumping or paw licking) was recorded. The specific testing sequence was chosen based on our prior studies showing that this order of testing reduced within-group variability and produced the most consistent results (Jackson et al., 2008). All studies were performed by an observer blinded to experimental treatment.

Cell Culture.

A549 and H460 NSCLC cells were maintained in DMEM supplemented with 10% (v/v) fetal bovine serum (FBS, Serum Source International, FB22-500HI, NC, USA) and 1% (v/v) combination of 10,000 U/ml penicillin and 10,000 μg/ml streptomycin (Pen/Strep, ThermoFisher Scientific, 15140–122, Carlsbad, CA), unless stated otherwise. Cells were incubated at 37°C under a humidified, 5% CO_2 atmosphere. The A549 and H460 cell lines were generously provided by the laboratories of Dr. Charles Chalfant and Dr. Richard Moran at VCU, respectively. The A549 and H460 cell lines were authenticated as exact matches for

the corresponding ATCC cell lines by the ATCC STR Cell Line Authentication Service in August of 2018.

Assessment of cell viability.

Cell viability was measured by either the MTT or MTS colorimetric assay or trypan blue exclusion. On the day of testing, the medium was removed, and cells were washed with PBS and stained with thiazolyl blue tetrazolium bromide (MTT, 2 mg/ml; Sigma-Aldrich, M2128, St. Louis, MO) in PBS for 3 hours. The MTT solution was then aspirated and replaced with DMSO. The color change was measured by a spectrophotometer (ELx800UV, BioTek, VT) at 490 nm. To avoid potentially aspirating cells, the CellTiter 96® Aqueous One Solution Cell Proliferation Assay (MTS; Promega, G358C, Madison, WI) was utilized for the less adherent A549 cell line. For trypan blue exclusion, cells were incubated with trypsin (0.25% trypsin-EDTA) for 3 minutes, stained with trypan blue (Invitrogen, 15250, Carlsbad, CA), and the viable, unstained cells were counted using a hemocytometer with bright-field microscopy.

Assessment of colony formation.

Cells were seeded at a low density in DMEM. Once the untreated control colonies reached a size of approximately 50 cells per colony, the samples were fixed with methanol, stained with crystal violet, and quantified (ColCount, Discovery Technologies International).

Assessment of apoptosis and DNA content.

Flow cytometry analyses were performed using BD FACSCanto II (BD Biosciences, San Jose, CA) and BD FACSDiva software at the Virginia Commonwealth University Flow Cytometry Core facility. For all studies, 10,000 cells per replicate within the gated region were analyzed. When collecting samples, both adherent and floating cells were harvested with 0.1% trypsin-EDTA and neutralized with medium after 48 hours of drug exposure. For quantification of apoptosis, cells were centrifuged and washed with PBS, then resuspended in 100 μl of 1x binding buffer with 5 μl of Annexin V and 5 μl of propidium iodide (BD Biosciences, FITC Annexin V Apoptosis Detection Kit, 556547, San Jose, CA). The samples were then incubated at room temperature while protected from light for 15 minutes. The suspension solution was then brought up to 500 μl using the 1x binding buffer and analyzed by flow cytometry. For quantification of DNA content, the cells were resuspended in 500 μl of a propidium iodide (PI) solution (50 μg/ml PI, 4 mM sodium citrate, 0.2 mg/ml DNase-free RNase A, and 0.1% Triton-X 100) for 1 hour at room temperature, while being protected from light (Tate et al., 1983). Before flow cytometry analysis, NaCl was added to the cell suspensions to achieve a final concentration of 0.20 M.

Assessment of tumor growth *in vivo*.

Male NSG mice were subcutaneously injected with 1.5×10^6 A549 NSCLC cells in both flanks. The A549 cells were collected via trypsinization, then neutralized with medium, centrifuged, and washed with PBS. Pellets of 1.5×10^6 A549 cells were then resuspended in 30 μl of 80% basement membrane extract (Trevigen, 3632-010-02, Gaithersburg, MD)/20% PBS. Mice were anesthetized with isoflurane (2% isoflurane/98% oxygen) via inhalation

during tumor cell inoculation; the injection site was swabbed with 70% ethanol prior to injection. Palpable tumors formed at approximately 20 days post-tumor cell inoculation, after which tumor volumes ($l \times w \times h$) were assessed with calipers every 2 to 3 days. Tumor volume was observed until humane endpoints were reached (tumor volume exceeds 1 cm3), at which time mice were euthanized via CO_2 asphyxiation followed by cervical dislocation. Tumors were then extracted, weighed, and preserved in 10% formalin.

Statistical Analyses

Data were analyzed using the GraphPad Prism software version 8.0.2 (GraphPad Software, Inc., La Jolla, CA) and expressed as the mean ± S.E.M. A three-way ANOVA with repeated measures was used to determine the overall interaction of the three factors (time, vehicle/paclitaxel treatment, distilled water/R-47 treatment) in the prevention study. A subsequent two-way ANOVA with repeated measures, followed by the Sidak post hoc test, was used to determine the difference between treatment groups at multiple time points in the reversal and prevention studies with R-47. An ordinary twoway ANOVA followed by the Sidak or Tukey post hoc tests were conducted in the R-47 tolerance, immunohistochemistry, and CPP studies as appropriate. For the *in vitro* lung cancer studies, one- and two-way ANOVAs were conducted and followed by the Bonferroni post hoc test. For the tumor-bearing animal study, a two-way linear mixed model was performed to account for missing values during delayed tumor growth (Toutenburg, 1991), and student's t-tests were performed to analyze tumor weight. All analyses were two-sided. Differences were considered significant at $P < 0.05$.

Results

R-47 Reverses Paclitaxel-Induced Mechanical Hypersensitivity

Acute administration of R-47 at doses of 1, 5, and 10 mg/kg p.o. reverses mechanical hypersensitivity in paclitaxel-treated mice in a time- and dose-dependent manner [$F_{dose \times time}$ (24, 168) = 14.92, $P < 0.0001$]; Figure 1A. The high and intermediate doses of R-47 (10 and 5 mg/kg) fully and partially reverse the mechanical hypersensitivity, respectively. However, administration of R-47 to vehicle-treated mice does not alter the mechanical threshold [$F_{dose \times time}$ (24, 168) = 0.3442, $P = 0.9984$]; Supplementary Figure 1. MLA, an α7 nAChR antagonist, significantly blocks the antinociceptive effect of R-47 in paclitaxel-treated mice [$F_{dose \times time}$ (6, 42) = 16.81, $P < 0.0001$; Figure 1B. In addition, sub-chronic administration of R-47 (10 mg/kg, p.o. twice daily for four days) does not produce tolerance to the reversal of mechanical hypersensitivity in paclitaxel-treated mice [$F_{dose \times time}$ (6, 42) = 33.41, $P <0.0001$]; Figure 1C.

R-47 Prevents Paclitaxel-Induced Mechanical Hypersensitivity and Intraepidermal Nerve Fiber Loss

In addition to the observed effect of R-47 in reversing mechanical hypersensitivity, chronic administration of R-47 (10 mg/kg p.o.) twice daily for three days prior to paclitaxel and twice daily during the paclitaxel regimen significantly prevents the development of mechanical hypersensitivity [$F_{paclitaxel \, or \, vehicle \times R\text{-}47 \, or \, vehicle \times days}$ (9,280) = 8.567, $P < 0.0001$]; Figure 2A. Comparing the vehicle-paclitaxel group to the vehicle-vehicle group reveals significant mechanical hypersensitivity due to paclitaxel treatment [$F_{dose \times time}$ (9,

63) = 19.4, P <0.0001]; Figure 2A. Comparing the R-47-paclitaxel-treated mice versus the vehicle-paclitaxel group demonstrates a significant antinociceptive effect of R-47 [$F_{dose \times time}$ (9, 63) = 25.1, P <0.0001]; Figure 2A.

To study whether R-47 has neuroprotective effects on the IENFs, R-47 (10 mg/kg, p.o.) or distilled water was administered to paclitaxel- or vehicle-treated mice. There is a significant interaction between paclitaxel and R-47 [$F_{paclitaxel \times R-47}$ (1, 20) = 27.85, P < 0.0001]; Figure 2B. As seen in Figures 2B and 2C, the vehicle-paclitaxel group of mice exhibits a significant reduction of IENFs compared to the vehicle-vehicle treated group (P < 0.0001). Importantly, the group of mice treated with R-47-paclitaxel demonstrates a significant increase of IENFs compared to vehicle-paclitaxel-treated mice (P < 0.0001).

R-47 Attenuates the Altered Morphology of Microglia induced by Paclitaxel

To investigate a potential role of microglia in our CIPN mouse model, we assessed the extent to which paclitaxel treatment alters the morphology of microglia in the lumbar spinal cord. The vehicle-paclitaxel group of mice demonstrates a significant decrease in stage I, which is the normal resting stage, characterized by long, thin, highly ramified processes. The vehicle-paclitaxel group also had an increase in stage III microglia (P < 0.0001), displaying more hypertrophic changes such as short, thickened processes and enlargement of the cell body. R-47 prevents the vehicle-paclitaxel-induced shift in the proportion of microglia in stage I versus stage III (P < 0.0001). There is a phenotypically subtle, but statistically significant interaction between paclitaxel and R-47 (10 mg/kg p.o.) in stage I (resting) and III (reactive) microglia morphology [$F_{paclitaxel \times R-47}$ (1, 20) = 101.7, P < 0.0001 and $F_{paclitaxel \times R-47}$ (1, 20) = 20.65; P < 0.0001, respectively]; Figure 3.

R-47 Does Not Induce Motor Deficits

To investigate whether R-47 would induce motor deficits in paclitaxel-treated mice, R-47 was administered at a dose of 10 mg/kg p.o., followed by testing in locomotor activity boxes and in the rotarod test. Importantly, R-47 does not show motor impairment in either test (Supplementary Table 1).

R-47 Induces Conditioned Place Preference (CPP) in Paclitaxel-Treated Mice

The CPP test was utilized to evaluate the ability of R-47 to induce preference in paclitaxel-treated mice, which can be interpreted as pain relief in mice experiencing ongoing, spontaneous pain (Navratilova et al., 2016). Administration of R-47 at a dose of 10 mg/kg p.o. induces significant CPP in paclitaxel-treated mice [$F_{paclitaxel \times R-47}$ (1, 56) = 5.4, P = 0.0238], but not in vehicle-treated mice; Figure 4.

Effects of R-47 on Nicotine CPP

We first evaluated the effect of R-47 pretreatment on the development of nicotine CPP in mice. For that, animals were pretreated with R-47 prior to nicotine on conditioning days. A two-way ANOVA revealed a significant rewarding effect for the nicotine treatment [F (1, 58) = 62.08, P<0.0001]; Figure 5. Pretreatment with R-47 at doses of (1 and 10 mg/kg; p.o) given 120 min prior to nicotine (0.5 mg/kg; s.c.), did not alter the rewarding effect of nicotine CPP and did not induce preference on its own in mice.

R-47 Does Not Precipitate Nicotine Withdrawal

The somatic and affective signs of nicotine withdrawal were determined in mice infused with 24 mg/kg nicotine per day via minipumps for 14 days. Nicotine withdrawal symptoms were assessed following administration of R-47, its vehicle, or mecamylamine on day 15. As seen in Figure 6, mecamylamine precipitated significant withdrawal symptoms in mice treated chronically with nicotine, including: an increases the number of somatic signs, [$F_{(1, 42)}$ = 39.90, P<0.0001]; Figure 6A, a decrease in hot plate latency, [$F_{(1, 42)}$ = 20.03 P<0.0001]; Figure 6B, and a reduction in time spent in the light chamber of the Light-Dark Box, [$F_{(1, 42)}$ = 4.847, P=0.0332]; Figure 6C, but no changes in the number of entries, [$F_{(1, 42)}$ = 0.8479, P=0.3624]; Figure 6D. Importantly, Tukey post hoc analysis revealed that R-47 does not precipitate withdrawal symptoms in all the aforementioned tests in nicotine-dependent mice (p>0.05); Figure 6A, B, C**, and** D.

R-47 Does Not Enhance Lung Tumor Cell Proliferation or Interfere with Sensitivity to Paclitaxel

Evidence in the scientific literature argues against the use of nicotine, a nAChR full agonist, within the framework of tumor growth or the utilization of cancer chemotherapy (Catassi et al., 2008; Grando, 2014). However, a closer examination of the data has revealed inconsistencies in both methodology and cancer growth outcomes, suggesting that further testing of nicotine and other nAChR agonists in the context of treating CIPN is necessary (Kyte and Gewirtz, 2018). Our previous work suggests that nicotine does not enhance lung tumor growth (Kyte et al., 2018); therefore, it is likely that a nAChR *silent* agonist would present an even lower risk of tumor growth stimulation. Dose-response cell viability and clonogenic assays were initially performed with R-47 to determine if the α7 silent agonist would affect NSCLC growth. The MTT cell viability and clonogenic assays revealed that R-47 (0.1–10 μM) does not significantly increase A549 and H460 cell growth (Supplementary Figures 2A **and** 3A). Likewise, R-47 does not affect NSCLC tumor cell growth under serum starvation and deprivation (0–5% FBS) conditions, which are typically used to synchronize the cell cycle and observe homogenous growth (Supplementary Figure 2B). Similarly, treatment with 1 μM R-47 did not cause an increase in NSCLC viable cell number for up to 7 days post-treatment when compared to untreated cells (Figure 7).

If R-47 is to be administered in conjunction with chemotherapy in the clinic, it is critical to establish that R-47 does not interfere with the antitumor activity of paclitaxel. To mimic the potential use of R-47 to reverse CIPN symptoms, NSCLC cells were exposed to paclitaxel followed by R-47. This sequential treatment regimen does not increase colony formation when compared to NSCLC cells treated with paclitaxel alone (Supplementary Figure 3B). Furthermore, when cells undergo R-47 pretreatment and subsequent co-treatment with paclitaxel to model the preventative use of R-47, the silent agonist does not interfere with the significant reduction in viable A549 or H460 cell number induced by paclitaxel alone (**insets of** Figure 7).

To further investigate the influence of R-47 on the growth inhibitory effects of paclitaxel, cell cycle analysis was performed following 48 hour-treatment with paclitaxel and/or R-47. Similar to the growth profile observed in Figure 7, the NSCLC cells co-treated with

paclitaxel and R-47 exhibit a significant increase in G2/M-arrested cells, as seen with paclitaxel alone (A549, P = 0.0004; H460, P < 0.0001 and A549, P = 0.0016, H460, P < 0.0001, respectively; Table 1).

In addition to growth arrest, paclitaxel is also known to promote programmed cell death or apoptosis (Jordan et al., 1996). According to Annexin V/Propidium Iodide (AV/PI) staining, R-47 does not induce apoptosis alone, nor does it significantly decrease paclitaxel-induced apoptosis (Figure 8). This observation is supported by the significant increase in fragmented DNA within the sub-G1 phase of the cell cycle following paclitaxel ± R-47 treatment (P < 0.0001; Table 1). Taken together, these *in vitro* studies indicate that the antitumor activity of paclitaxel is not compromised by R-47 (1 μM).

To test whether these *in vitro* findings translate to an animal cancer model, A549 NSCLC cells were subcutaneously injected into the flanks of male NSG mice. Once the tumors were established, R-47 (10 mg/kg, p.o.) was administered twice daily for 3 days, then once daily in combination with paclitaxel (10 mg/kg, i.p.) for 4 days. The paclitaxel regimen significantly decreases tumor volume when compared to vehicle-treated mice (P = 0.021; Figure 9A). Most importantly, R-47 does not increase tumor volume either alone or in combination with paclitaxel when compared to vehicle- and paclitaxel-treated mice, respectively. Likewise, the tumor weights followed the same trend, with R-47 having no significant effect alone or when administered with paclitaxel (Figure 9B). These *in vivo* data suggest that R-47 will most likely not affect lung tumor growth when administered prior to and during cancer chemotherapy to prevent chemotherapy-induced peripheral neuropathy.

Discussion

This is the first study to identify that targeting the α7 nAChR with the selective silent agonist R-47 reverses and prevents CIPN induced by paclitaxel in mice. Acute administration of R-47 dose- and time-dependently shows an antinociceptive effect in paclitaxel-treated mice but not in vehicle-treated mice. Furthermore, this antinociceptive effect is consistent with a recent report showing that administration of the selective silent agonist NS6740 reverses mechanical hypersensitivity in mice with a chronic constriction injury (CCI), a model of neuropathic pain (Papke et al., 2015). Consistent with our previous reports (Kyte et al., 2018; Toma et al., 2017) and the reports of others (Curry et al., 2018; Donvito et al., 2016; Legakis et al., 2018; Legakis and Negus, 2018; Makker et al., 2017), paclitaxel induces mechanical hypersensitivity in rodents.

The administration of MLA, an α7 nAChR antagonist, blocked the antinociceptive effect of R-47, indicating that the effect is mediated by an α7 nAChR-dependent mechanism. Moreover, the sub-chronic administration of R-47 does not produce tolerance to the antinociceptive effect in paclitaxel-treated mice, which is in contrast to other known antinociceptive/analgesic drugs, such as morphine, which induces tolerance after repeated administration in mice (Lin et al., 2018) and rats (Legakis and Negus, 2018) treated with paclitaxel.

Consistent with other reports in the literature (Krukowski et al., 2015; Park et al., 2015; Turkiew et al., 2017), our results show that paclitaxel-treated mice have a reduction in IENF density (Toma et al., 2017). We previously demonstrated that nicotine, a non-selective nAChRs agonist, prevents the reduction of IENF caused by paclitaxel (Kyte et al., 2018). In our current study, we show that chronic administration of R-47, a selective α7 nAChR agonist, was able to recapitulate these results, when administered at a dose of 10 mg/kg p.o., prior to and during paclitaxel treatment. Protection of IENF by R-47 lasts for the duration of the study, up to 35 days. Further, R-47 prevents the development of mechanical hypersensitivity in mice. It is important to note that paclitaxel did cause motor impairment in mice, which we observed previously (Toma et al., 2017). Additionally, we are the first to report the effects of R-47 in the rotarod test and locomotor activity test; R-47 did not impair motor coordination in either test (Supplementary Table 1).

When an injury occurs, microglia become activated and release pro-inflammatory cytokines and chemokines, which stimulate secondary nociceptive neurons and enhance pain chronification (Salter and Stevens, 2017). Here, we show that paclitaxel-treated mice exhibit a shift in microglia morphology from stage I to stage III, suggesting a change from resting to a reactive state. (Shen et al., 2015) report a similar shift in spinal microglia morphology after treatment with vincristine in mice, and (Di Cesare Mannelli et al., 2014b) also report microglia activation at day 7 in a rat model of oxaliplatin-induced neuropathy. Further, other studies in rats (Burgos et al., 2012; Peters et al., 2007; Wu et al., 2018) and mice (Makker et al., 2017; Ruiz-Medina et al., 2013) show that paclitaxel causes activation of spinal microglia. Together, these findings suggest that various chemotherapeutics can induce phenotypic changes in spinal microglia.

Conversely, several authors did not see activation of microglia in the spinal cord in rodent models in response to vincristine (Ji et al., 2013), oxaliplatin (Di Cesare Mannelli et al., 2014b, 2014a), bortezomib (Robinson et al., 2014), or paclitaxel (Zhang et al., 2012) chemotherapeutic treatment. The discrepancies between authors could be due to many variables, such as species, sex, age, chemotherapeutic agent, route of administration, dosing regimen, cumulative dose, and time course of the study.

In the current study, we observe that R-47 prevents alterations in microglial morphology in paclitaxel-treated mice. There is limited published research on the effects of α7 modulators on microglia in paclitaxel-treated rodents. While (Di Cesare Mannelli et al., 2014a) report that the DNA-alkylating antineoplastic oxaliplatin did not induce phenotypical changes in spinal microglia morphology in rats, the authors did note that oxaliplatin was sufficient to induce astrocytic activation in the spinal cord. The same authors were able to demonstrate that the full α7 agonist PNU282987 was able to neutralize this activation, as well as reverse and prevent neuropathy. Further, (St-Pierre et al., 2016) show that stimulation of nAChRs in mouse bone marrow with the nonselective agonist nicotine has anti-inflammatory effects, and these anti-inflammatory effects are absent in α7 KO mice, supporting the role of α7 modulation in rodent models of inflammation.

Injury causes activation of microglia, producing phenotypic changes and release of pro-inflammatory cytokines. α7 stimulation on microglia leads to activation of Janus Kinase 2

(Jak2) signaling, which, in turn, activates signal transducer and activator of transcription 3 (Stat3), leading to inhibition of NF-κB translocation to the nucleus, ultimately suppressing transcription and release of pro-inflammatory cytokines (Egea et al., 2015). Indirect inhibition of NF-κB by R-47 could explain the decrease in reactive microglia observed in the paclitaxel-R-47 group.

Ligands that target α7 nAChRs can bind to different sites, producing a variety of effects on the receptors' conformational dynamics. Orthosteric α7 agonists promote channel activation; however, orthosteric activation of α7 is not sufficient to explain the diverse effects of α7 "activation" on the cholinergic anti-inflammatory pathway. In particular, immune cells in the cholinergic anti-inflammatory pathway without channel-dependent signaling respond to α7 ligands. This has led to the hypothesis that α7 signaling can be mediated by a desensitized, non-conducting state of the receptor. Consistent with this proposed mechanism, a class of extremely weak, partial agonists for α7 is associated with the cholinergic anti-inflammatory pathway. Such ligands that stabilize a sensitive-desensitized, non-conducting state are identified as "silent agonists" (Horenstein and Papke, 2017). The effective induction of the non-conduction states is what distinguishes a silent agonist from a molecule that is simply a poor activator of the channel, and this distinction can be confirmed with the use of positive allosteric modulators that destabilize non-conducting states (Papke et al., 2015). Similar to silent agonists, full α7 agonists, such as PNU-282987, ultimately promote and stabilize non-conducting receptor conformations, which is consistent with the anti-inflammatory effects of PNU-282987 reported by (Di Cesare Mannelli et al., 2014a).

Our studies also reveal that R-47 promotes preference in the CPP test in paclitaxel-treated mice, suggesting that R-47 produces relief from both pain and an aversive state in paclitaxel-treated mice. Our results are consistent with another study that used the CPP test to assess potential CIPN interventions. For example, administration of MJN110 (5 mg/kg, i.p.), an endocannabinoid monoacylglycerol lipase inhibitor, produces CPP in paclitaxel-treated mice but not in vehicle-treated mice (Curry et al., 2018). Importantly and in contrast to several drugs of abuse, such as nicotine (Jackson et al., 2017) and morphine (Neelakantan et al., 2016), R-47 does not show preference in the CPP test in vehicle-treated mice, suggesting that R-47 lacks the intrinsic rewarding properties of drugs that have abuse liability. Our lab and others have previously shown that nicotine induces a rewarding effect in the CPP test and produces physical and affective withdrawal symptoms (Jackson et al., 2015; Kallupi and George, 2017). Importantly, R-47 neither alters the rewarding effect of nicotine nor precipitates nicotine's withdrawal symptoms. Furthermore, the selectivity of R-47 to α7 nAChR subtypes may decrease the possibility of adverse events, observed with nicotine patch use, which can induce nausea and respiratory symptoms (Greenland et al., 1998).

These observations led us to investigate if R-47 would influence cancer progression before and/or during chemotherapy, especially considering the controversy surrounding the role of nicotine, a nAChR full agonist, in cancer growth (Kyte and Gewirtz, 2018). Consistent with our previous work involving nicotine (Kyte et al., 2018), concentrations of R-47 that alleviate mechanical hypersensitivity do not appear to promote lung cancer progression in our cell culture and tumor-bearing animal models. For example, mice receiving 5 mg/kg

R-47 orally, a dose shown in Figure 1 to partially reverse paclitaxel-induced mechanical hypersensitivity, have a C_{max} of 324 ng/ml or 0.78 μM (Clark et al., 2014), which is similar to our *in vitro* R-47 concentration of 1 μM. A higher dose of R-47 (10 mg/kg, p.o.) that fully reverses and prevents paclitaxel-induced hypersensitivity was used in our tumor-bearing animal studies (Figures 1, 2**, and** 9).

Currently, the α7 nAChR is thought to play a role in the nAChR-mediated promotion of cancer cell proliferation and survival. For example, Mucchietto et al show that nicotine significantly increases A549 cell number, which is inhibited by the α7 nAChR antagonists α-bungarotoxin and MLA (Mucchietto et al., 2017). However, our data demonstrate that the α7 nAChR silent agonist R-47 does not promote NSCLC growth or interfere with paclitaxel-induced growth arrest and apoptosis. Although the full mechanism of action of R-47 is currently unknown, the lack of effect of R-47 could be due to the fact that the silent agonist is stabilizing the sensitive desensitized form of the α7 nAChR and thus preventing endogenous acetylcholine from binding. Furthermore, R-47 may serve as a functional antagonist after the initial receptor response, with no detectable inhibition of paclitaxel's antitumor effects. Collectively, our results support the development of α7 nAChR silent agonists, such as R-47, as promising therapies for CIPN.

Supplementary Material

Refer to Web version on PubMed Central for supplementary material.

Acknowledgements

References

Bagdas D, AlSharari SD, Freitas K, Tracy M, Damaj MI, 2015 The role of alpha5 nicotinic acetylcholine receptors in mouse models of chronic inflammatory and neuropathic pain. Biochem. Pharmacol 97, 590–600. doi:10.1016/j.bcp.2015.04.013 [PubMed: 25931144]

Bagdas D, Gurun MS, Flood P, Papke RL, Damaj MI, 2017 New Insights on Neuronal Nicotinic Acetylcholine Receptors as Targets for Pain and Inflammation: A Focus on α7 nAChRs. Curr. Neuropharmacol doi:10.2174/1570159X15666170818102108

Bencherif M, Lippiello PM, Lucas R, Marrero MB, 2011 Alpha7 nicotinic receptors as novel therapeutic targets for inflammation-based diseases. Cell. Mol. Life Sci 68, 931–949. doi:10.1007/s00018-010-0525-1 [PubMed: 20953658]

Briggs CA, Grønlien JH, Curzon P, Timmermann DB, Ween H, Thorin-Hagene K, Kerr P, Anderson DJ, Malysz J, Dyhring T, Olsen GM, Peters D, Bunnelle WH, Gopalakrishnan M, 2009 Role of channel activation in cognitive enhancement mediated by alpha-7 nicotinic acetylcholine receptors. Br. J. Pharmacol 158, 1486–1494. doi:10.1111/j.1476-5381.2009.00426.x [PubMed: 19845675]

Burgos E, Gómez-Nicola D, Pascual D, Martín I, Nieto-Sampedro M, Goicoechea C, 2012 Cannabinoid agonist WIN 55,212–2 prevents the development of paclitaxel-induced peripheral

neuropathy in rats. Possible involvement of spinal glial cells. Eur. J. Pharmacol 682, 62–72. doi: 10.1016/j.ejphar.2012.02.008 [PubMed: 22374260]

Catassi A, Servent D, Paleari L, Cesario A, Russo P, 2008 Multiple roles of nicotine on cell proliferation and inhibition of apoptosis: Implications on lung carcinogenesis. Mutat. Res. - Rev. Mutat. Res 659, 221–231. doi:10.1016/j.mrrev.2008.04.002

Chaplan SR, Bach FW, Pogrel JW, Chung JM, Yaksh TL, 1994 Quantitative assessment of tactile allodynia in the rat paw. J. Neurosci. Methods 53, 55–63. doi:10.1016/0165-0270(94)90144-9 [PubMed: 7990513]

Chen G, Zhang YQ, Qadri YJ, Serhan CN, Ji RR, 2018 Microglia in Pain: Detrimental and Protective Roles in Pathogenesis and Resolution of Pain. Neuron 100, 1292–1311. doi:10.1016/j.neuron. 2018.11.009 [PubMed: 30571942]

Clark RB, Lamppu D, Libertine L, McDonough A, Kumar A, LaRosa G, Rush R, Elbaum D, 2014 Discovery of novel 2-((pyridin-3-yloxy)methyl)piperazines as α7 nicotinic acetylcholine receptor modulators for the treatment of inflammatory disorders. J. Med. Chem 57, 3966–3983. doi:10.1021/ jm5004599 [PubMed: 24814197]

Cordero-Erausquin M, Pons S, Faure P, Changeux JP, 2004 Nicotine differentially activates inhibitory and excitatory neurons in the dorsal spinal cord. Pain 109, 308–318. doi:10.1016/j.pain. 2004.01.034 [PubMed: 15157692]

Curry Z, Wilkerson J, Bagdas D, Kyte S, Patel N, Donvito G, Mustafa MA, Poklis J, Niphakis M, Hsu K-L, Cravatt BF, Gewirtz DA, Damaj MI, Lichtman AH, 2018 Monoacylglycerol lipase inhibitors reverse paclitaxel-induced nociceptive behavior and proinflammatory markers in a mouse model of chemotherapy-induced neuropathy. J. Pharmacol. Exp. Ther. jpet.117.245704 doi:10.1124/jpet. 117.245704

Di Cesare Mannelli L, Pacini A, Matera C, Zanardelli M, Mello T, De Amici M, Dallanoce C, Ghelardini C, 2014a Involvement of α7 nAChR subtype in rat oxaliplatin-induced neuropathy: Effects of selective activation. Neuropharmacology 79, 37–48. doi:10.1016/j.neuropharm. 2013.10.034 [PubMed: 24225197]

Di Cesare Mannelli L, Pacini A, Micheli L, Tani A, Zanardelli M, Ghelardini C, 2014b Glial role in oxaliplatin-induced neuropathic pain. Exp. Neurol 261, 22–33. doi:10.1016/j.expneurol. 2014.06.016 [PubMed: 24967684]

Di Cesare Mannelli L, Zanardelli M, Ghelardini C, 2013 Nicotine is a pain reliever in trauma- and chemotherapy-induced neuropathy models. Eur. J. Pharmacol 711, 87–94. doi:10.1016/j.ejphar. 2013.04.022 [PubMed: 23648560]

Donvito G, Wilkerson JL, Damaj MI, Lichtman AH, 2016 Palmitoylethanolamide Reverses Paclitaxel-Induced Allodynia in Mice. J. Pharmacol. Exp. Ther 359, 310–318. doi:10.1124/jpet.116.236182 [PubMed: 27608657]

Egea J, Buendia I, Parada E, Navarro E, León R, Lopez MG, 2015 Anti-inflammatory role of microglial alpha7 nAChRs and its role in neuroprotection. Biochem. Pharmacol 97, 463–472. doi: 10.1016/j.bcp.2015.07.032 [PubMed: 26232730]

Ewertz M, Qvortrup C, Eckhoff L, 2015 Chemotherapy-induced peripheral neuropathy in patients treated with taxanes and platinum derivatives. Acta Oncol. (Madr) 54, 587–591. doi: 10.3109/0284186X.2014.995775

Freitas K, Ghosh S, Ivy Carroll F, Lichtman AH, Imad Damaj M, 2013 Effects of alpha 7 positive allosteric modulators in murine inflammatory and chronic neuropathic pain models. Neuropharmacology 65, 156–164. doi:10.1016/j.neuropharm.2012.08.022 [PubMed: 23079470]

Grabus SD, Carroll FI, Damaj MI, 2012 Bupropion and its main metabolite reverse nicotine chronic tolerance in the mouse. Nicotine Tob. Res 14, 1356–1361. doi:10.1093/ntr/nts088 [PubMed: 22589419]

Grando S.a, 2014 Connections of nicotine to cancer. Nat. Rev. Cancer 14, 419–429. doi:10.1038/ nrc3725 [PubMed: 24827506]

Greenland S, Satterfield MH, Lanes SF, 1998 A meta-analysis to assess the incidence of adverse effects associated with the transdermal nicotine patch. Drug Saf 18, 297–308. [PubMed: 9565740]

Hagiwara H, Sunada Y, 2004 Mechanism of taxane neurotaxicity. Breast Cancer 11, 82–85. doi: 10.1007/BF02968008 [PubMed: 14718798]

Horenstein NA, Papke RL, 2017 Anti-inflammatory Silent Agonists. ACS Med. Chem. Lett 8, 989–991. doi:10.1021/acsmedchemlett.7b00368 [PubMed: 29057037]

Jackson A, Bagdas D, Muldoon PP, Lichtman AH, Carroll FI, Greenwald M, Miles MF, Damaj MI, 2017 In vivo interactions between α7 nicotinic acetylcholine receptor and nuclear peroxisome proliferator-activated receptor-α: Implication for nicotine dependence. Neuropharmacology 118, 38–45. doi:10.1016/j.neuropharm.2017.03.005 [PubMed: 28279662]

Jackson KJ, Martin BR, Changeux JP, Damaj MI, 2008 Differential Role of Nicotinic Acetylcholine Receptor Subunits in Physical and Affective Nicotine Withdrawal Signs. J. Pharmacol. Exp. Ther 325, 302–312. doi:10.1124/jpet.107.132977 [PubMed: 18184829]

Jackson KJ, Muldoon PP, De Biasi M, Damaj MI, 2015 New mechanisms and perspectives in nicotine withdrawal. Neuropharmacology 96, 223–234. doi:10.1016/j.neuropharm.2014.11.009 [PubMed: 25433149]

Ji XT, Qian NS, Zhang T, Li JM, Li XK, Wang P, Zhao DS, Huang G, Zhang L, Fei Z, Jia D, Niu L, 2013 Spinal Astrocytic Activation Contributes to Mechanical Allodynia in a Rat Chemotherapy-Induced Neuropathic Pain Model. PLoS One 8, 2–13. doi:10.1371/journal.pone.0060733

Kallupi M, George O, 2017 Nicotine Vapor Method to Induce Nicotine Dependence in Rodents, in: Current Protocols in Neuroscience John Wiley & Sons, Inc., Hoboken, NJ, USA, pp. 8.41.1–8.41.10. doi:10.1002/cpns.34

Krukowski K, Nijboer CH, Huo X, Kavelaars A, Heijnen CJ, 2015 Prevention of chemotherapy-induced peripheral neuropathy by the small-molecule inhibitor pifithrin-[mu]. Pain 156, 2184–2192. [PubMed: 26473292]

Kyte SL, Gewirtz DA, 2018 The Influence of Nicotine on Lung Tumor Growth, Cancer Chemotherapy, and Chemotherapy-Induced Peripheral Neuropathy. J. Pharmacol. Exp. Ther 366, 303–313. doi:10.1124/jpet.118.249359 [PubMed: 29866790]

Kyte SL, Toma W, Bagdas D, Meade JA, Schurman LD, Lichtman AH, Chen Z-J, Del Fabbro E, Fang X, Bigbee JW, Damaj MI, Gewirtz DA, 2018 Nicotine Prevents and Reverses Paclitaxel-Induced Mechanical Allodynia in a Mouse Model of CIPN. J. Pharmacol. Exp. Ther 364, 110–119. doi:10.1124/jpet.117.243972 [PubMed: 29042416]

Legakis LP, Bigbee JW, Negus SS, 2018 Lack of paclitaxel effects on intracranial self-stimulation in male and female rats. Behav. Pharmacol 29, 290–298. doi:10.1097/FBP.0000000000000378 [PubMed: 29369054]

Legakis LP, Negus SS, 2018 Repeated Morphine Produces Sensitization to Reward and Tolerance to Antiallodynia in Male and Female Rats with Chemotherapy-Induced Neuropathy. J. Pharmacol. Exp. Ther 365, 9–19. doi:10.1124/jpet.117.246215 [PubMed: 29363579]

Lin X, Dhopeshwarkar AS, Huibregtse M, Mackie K, Hohmann AG, 2018 Slowly Signaling G Protein – Biased CB 2 Cannabinoid Receptor Agonist LY2828360

Suppresses Neuropathic Pain with Sustained Efficacy and Attenuates Morphine Tolerance and Dependences. Mol Pharmacol 93, 49–62. doi:10.1124/mol.117.109355

Makker PGS, Duffy SS, Lees JG, Perera CJ, Tonkin RS, Butovsky O, Park SB, Goldstein D, Moalem-Taylor G, 2017 Characterisation of immune and neuroinflammatory changes associated with chemotherapy-induced peripheral neuropathy. PLoS One 12, e0170814. doi:10.1371/journal.pone.0170814 [PubMed: 28125674]

Mcmahon SB, La Russa F, Bennett DLH, 2015 Crosstalk between the nociceptive and immune systems in host defence and disease. Nat. Rev. Neurosci 16, 389–402. doi:10.1038/nrn3946 [PubMed: 26087680]

Mucchietto V, Fasoli F, Pucci S, Moretti M, Benfante R, Maroli A, Di Lascio S, Bolchi C, Pallavicini M, Dowell C, Mcintosh M, Clementi F, Gotti C, 2017 α9- and α7-containing receptors mediate the pro-proliferative effects of nicotine in the A549 adenocarcinoma cell line. Br. J. Pharmacol doi:10.1111/bph.13954

Navratilova E, Morimura K, Xie JY, Atcherley CW, Ossipov MH, Porreca F, 2016 Positive emotions and brain reward circuits in chronic pain. J. Comp. Neurol 524, 1646–1652. doi:10.1002/cne.23968 [PubMed: 26788716]

Neelakantan H, Ward SJ, Walker EA, 2016 Effects of paclitaxel on mechanical sensitivity and morphine reward in male and female C57Bl6 mice. Exp. Clin. Psychopharmacol 24, 485–495. doi: 10.1037/pha0000097 [PubMed: 27929349]

Papke RL, Bagdas D, Kulkarni AR, Gould T, Alsharari SD, Thakur GA, Damaj MI, 2015 The analgesic-like properties of the alpha7 nAChR silent agonist NS6740 is associated with non-conducting conformations of the receptor. Neuropharmacology 91, 34–42. doi:10.1016/j.neuropharm.2014.12.002 [PubMed: 25497451]

Papke RL, Stokes C, Damaj MI, Thakur GA, Manther K, Treinin M, Bagdas D, Kulkarni AR, Horenstein NA, 2018 Persistent activation of α7 nicotinic ACh receptors associated with stable induction of different desensitized states. Br. J. Pharmacol 175, 1838–1854. doi:10.1111/bph.13851 [PubMed: 28477386]

Park JS, Kim S, Hoke A, 2015 An exercise regimen prevents development paclitaxel induced peripheral neuropathy in a mouse model. J. Peripher. Nerv. Syst 20, 7–14. doi:10.1111/jns.12109 [PubMed: 25858462]

Peters CM, Jimenez-Andrade JM, Jonas BM, Sevcik M. a., Koewler NJ, Ghilardi JR, Wong GY, Mantyh PW, 2007 Intravenous paclitaxel administration in the rat induces a peripheral sensory neuropathy characterized by macrophage infiltration and injury to sensory neurons and their supporting cells. Exp. Neurol 203, 42–54. doi:10.1016/j.expneurol.2006.07.022 [PubMed: 17005179]

Richner M, Jager SB, Siupka P, Vaegter CB, 2017 Hydraulic Extrusion of the Spinal Cord and Isolation of Dorsal Root Ganglia in Rodents. J. Vis. Exp 1–6. doi:10.3791/55226

Robinson CR, Zhang H, Dougherty PM, 2014 Astrocytes, but not microglia, are activated in oxaliplatin and bortezomib-induced peripheral neuropathy in the rat. Neuroscience 274, 308–317. doi:10.1016/j.neuroscience.2014.05.051 [PubMed: 24905437]

Ruiz-Medina J, Baulies A, Bura SA, Valverde O, 2013 Paclitaxel-induced neuropathic pain is age dependent and devolves on glial response. Eur. J. Pain (United Kingdom) 17, 75–85. doi:10.1002/j.1532-2149.2012.00172.x

Salter MW, Stevens B, 2017 Microglia emerge as central players in brain disease. Nat. Med 23, 1018–1027. doi:10.1038/nm.4397 [PubMed: 28886007]

Shen Y, Zhang Z-J, Zhu M-D, Jiang B-C, Yang T, Gao Y-J, 2015 Exogenous induction of HO-1 alleviates vincristine-induced neuropathic pain by reducing spinal glial activation in mice. Neurobiol. Dis 79, 100–110. doi:10.1016/j.nbd.2015.04.012 [PubMed: 25956228]

St-Pierre S, Jiang W, Roy P, Champigny C, LeBlanc É, Morley BJ, Hao J, Simard AR, 2016 Nicotinic Acetylcholine Receptors Modulate Bone Marrow-Derived Pro-Inflammatory Monocyte Production and Survival. PLoS One 11, e0150230. doi:10.1371/journal.pone.0150230 [PubMed: 26925951]

Tate EH, Wilder ME, Cram LS, Wharton W, 1983 A method for staining 3T3 cell nuclei with propidium iodide in hypotonic solution. Cytometry 4, 211–215. doi:10.1002/cyto.990040304 [PubMed: 6198128]

Toma W, Kyte SL, Bagdas D, Alkhlaif Y, Alsharari SD, Lichtman AH, Chen Z-J, Del Fabbro E, Bigbee JW, Gewirtz DA, Damaj MI, 2017 Effects of paclitaxel on the development of neuropathy and affective behaviors in the mouse. Neuropharmacology 117, 305–315. doi:10.1016/j.neuropharm.2017.02.020 [PubMed: 28237807]

Toutenburg H, 1991 Little RJA. and Rubin DB:Statistical analysis with missing data. Stat. Pap 32, 70–70. doi:10.1007/BF02925480

Tracey KJ, 2002 The inflammatory reflex –. Nature 420, 835–859. doi:10.1111/j.1365-2796.2004.01440.x

Turkiew E, Falconer D, Reed N, Höke A, 2017 Deletion of Sarm1 gene is neuroprotective in two models of peripheral neuropathy. J. Peripher. Nerv. Syst 22, 162–171. doi:10.1111/jns.12219 [PubMed: 28485482]

van Maanen MA, Papke RL, Koopman FA, Koepke J, Bevaart L, Clark R, Lamppu D, Elbaum D, LaRosa GJ, Tak PP, Vervoordeldonk MJ, 2015 Two Novel α7 Nicotinic Acetylcholine Receptor Ligands: In Vitro Properties and Their Efficacy in Collagen-Induced Arthritis in Mice. PLoS One 10, e0116227. doi:10.1371/journal.pone.0116227 [PubMed: 25617631]

Wu J, Hocevar M, Bie B, Foss JF, Naguib M, 2018 Cannabinoid Type 2 Receptor System Modulates Paclitaxel-Induced Microglial Dysregulation and Central Sensitization in Rats. J. Pain 00. doi: 10.1016/j.jpain.2018.10.007

Zhang Haijun, Yoon S-Y, Zhang Hongmei, Dougherty PM, 2012 Evidence That Spinal Astrocytes but Not Microglia Contribute to the Pathogenesis of Paclitaxel-Induced Painful Neuropathy. J. Pain 13, 293–303. doi:10.1016/j.jpain.2011.12.002 [PubMed: 22285612]

Zheng FY, Xiao WH, Bennett GJ, 2011 The response of spinal microglia to chemotherapy-evoked painful peripheral neuropathies is distinct from that evoked by traumatic nerve injuries. Neuroscience 176, 447–454. doi:10.1016/j.neuroscience.2010.12.052 [PubMed: 21195745]

- α7 silent agonist R-47 is antinociceptive in mice

- R-47 suppresses paclitaxel-induced changes in spinal microglia morphology

- R-47 lacks rewarding effects but produces spontaneous pain relief in the CPP test

- R-47 does not precipitate nicotine physical and affective-like withdrawal symptoms

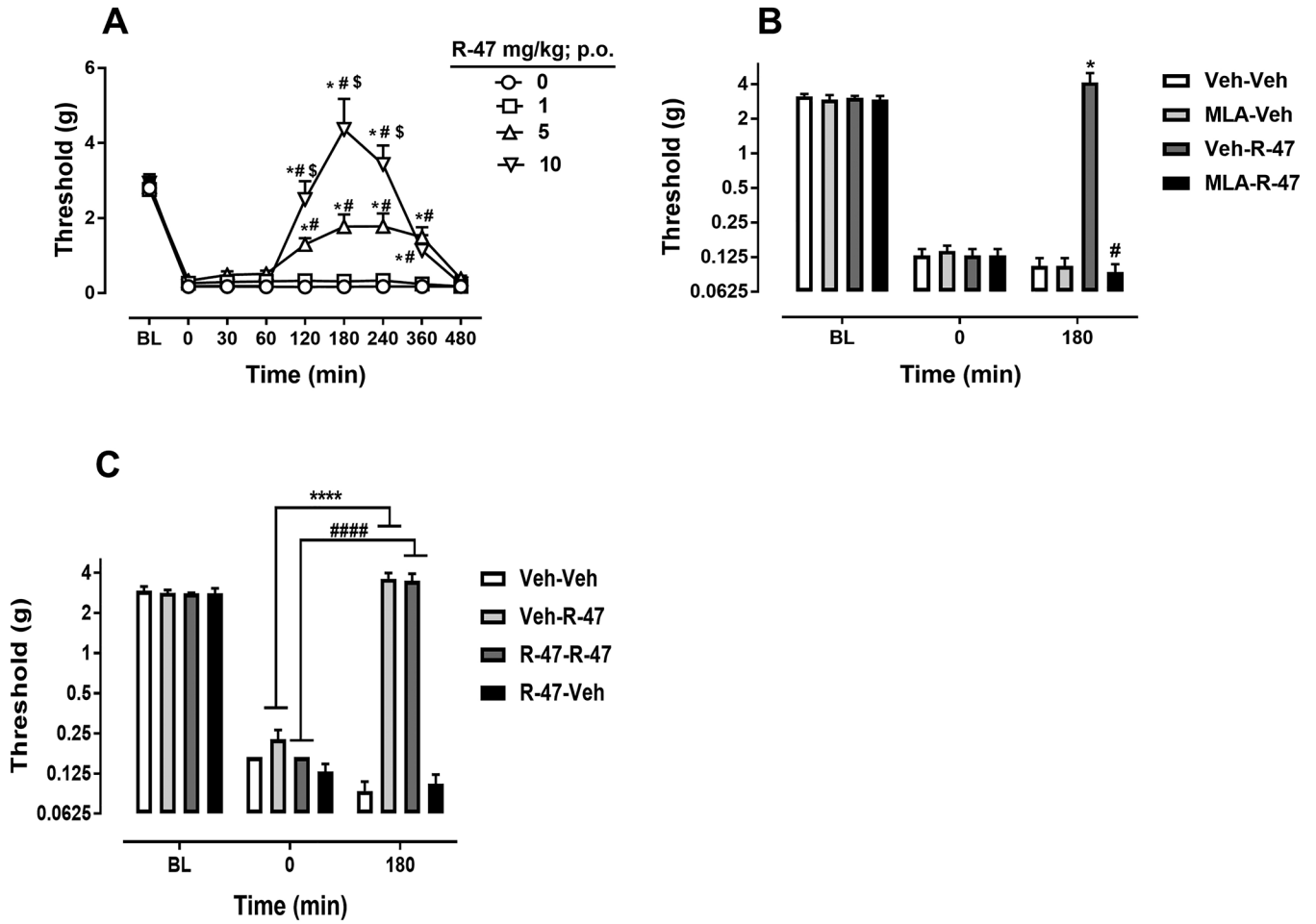- R-47 does not enhance tumor growth nor impair paclitaxel's antitumor effects

Figure 1.

R-47 reverses CIPN in mice in an α7-dependent manner with no development of tolerance. A) Acute administration of R-47 at doses of 1, 5, and 10 mg/kg p.o. reverses mechanical hypersensitivity in paclitaxel-treated mice. *P < 0.0001 vs distilled water (0 mg/kg); #P < 0.0001 vs R-47 (1 mg/kg); $P < 0.0001 vs R-47 (5 mg/kg). B) Administration of MLA, an α7 nAChR antagonist, at a dose of 10 mg/kg s.c. 10 minutes before R-47 (10 mg/kg, p.o.) blocks the antinociceptive effect of R-47 in paclitaxel-treated mice. *P < 0.0001 Veh-R-47 at 180 min vs 0 min; #P < 0.0001 MLA-R-47 vs Veh-R-47 at 180 min. C) Administration of R-47 at a dose of 10 mg/kg p.o. for four days and on day 5 (challenge day) shows the antinociceptive effect in paclitaxel-treated mice. *P < 0.0001 Veh-R-47 at 180 min vs 0 min; #P < 0.0001 R-47-R-47 at 180 vs R-47-R-47 at 0 min. BL, Baseline; Veh, vehicle; Pac, paclitaxel; MLA, methyllycaconitine; n = 8 per group; data expressed as mean ± SEM.
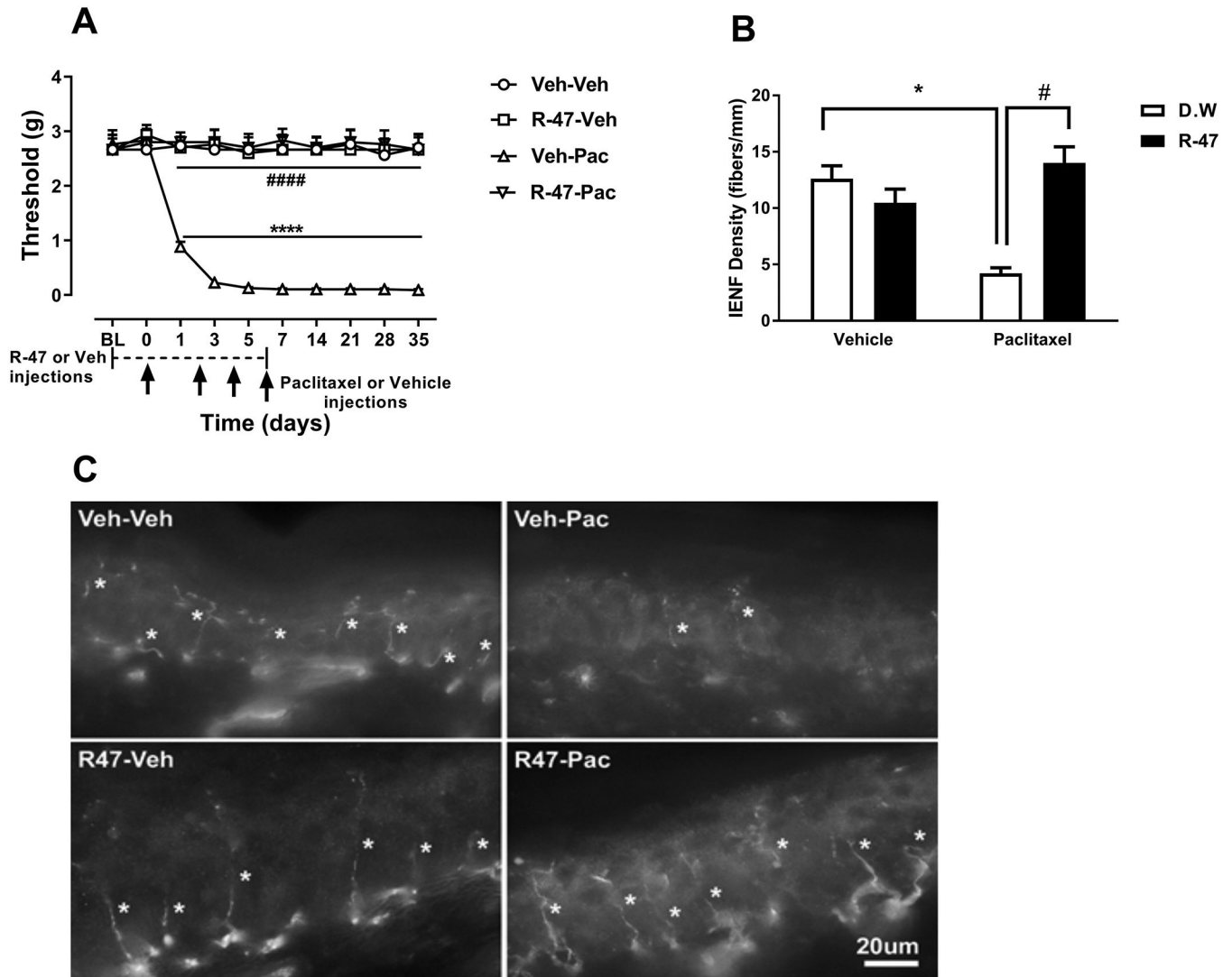
Figure 2.

R-47 prevents CIPN in mice. A) Chronic administration of R-47 at a dose of 10 mg/kg p.o. completely prevents the development of mechanical hypersensitivity. **** $P < 0.0001$ Veh-Veh vs Veh-Pac; #### $P < 0.0001$ R-47-Pac vs Veh-Pac; BL, baseline; Veh, Vehicle; Pac, Paclitaxel. n=8 per group; Data expressed as mean ± SEM. B) Mice injected with paclitaxel at a dose of 8 mg/kg i.p. for one cycle demonstrate a significant reduction of IENFs at 35 days post-paclitaxel injection. However, pre- and co-administration of R-47 at a dose of 10 mg/kg p.o. to paclitaxel-treated mice completely prevents the reduction of IENFs; *$P < 0.0001$ D.W.-paclitaxel vs D.W.-vehicle; #$P < 0.0001$ R-47-paclitaxel vs D.W.-paclitaxel. C) Immunostained sections of hind paw epidermis represent the reduction of IENF density by paclitaxel and protection by R-47. Bar represents 20 microns in all images. Images were captured under 63x magnification. IENFs, intra-epidermal nerve fibers; D.W., distilled water. Asterisks denote IENFs. n = 6 per group; data expressed as mean ± SEM.
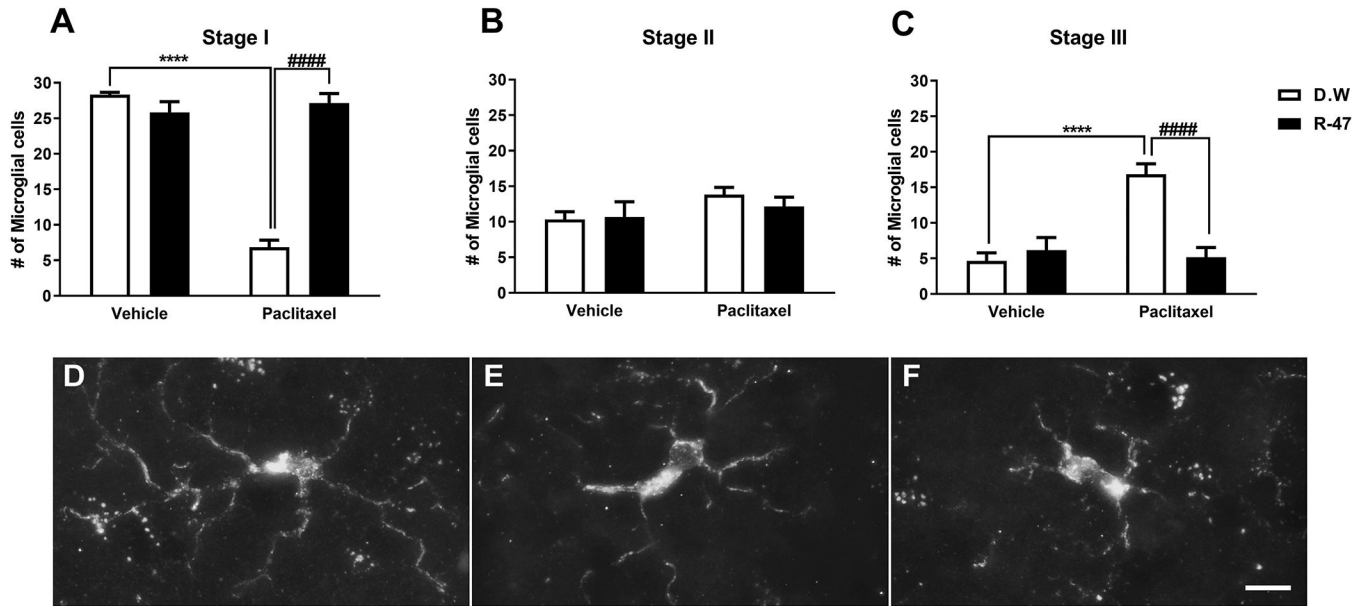
Figure 3.

R-47 prevents paclitaxel-induced alterations in dorsal horn microglia. (A) Mice injected with paclitaxel (8 mg/kg i.p. for one cycle) plus distilled water (D.W., the vehicle for R-47) reveal a significant decrease in the number of stage I microglial cells at 35 days post-paclitaxel injection, which was prevented by pre-and co-administration of R-47 at a dose of 10 mg/kg p.o. (C) Mice injected with paclitaxel plus D.W. show a significant elevation in the number of stage III microglial cells, which was prevented by pre-and co-administration of R-47. (B) There were no significant changes in the number of stage II microglial cells between the treatment groups. (D-F) Representative images of microglial stages: (D) Stage I, cells with long, thin, and highly ramified processes; (E) Stage II, cells with shorter, thickened processes with less branching; and (F) Stage III, cells with increased hypertrophic changes such as shorter, thickened processes and cell body enlargement. ****$P < 0.0001$ D.W.-paclitaxel vs D.W.-vehicle; ####$P < 0.0001$ R-47-paclitaxel vs D.W.-paclitaxel. Bar represents 10 microns in all images. Images were captured under 63x magnification. D.W., distilled water. $n = 6$ per group; data expressed as mean ± SEM.
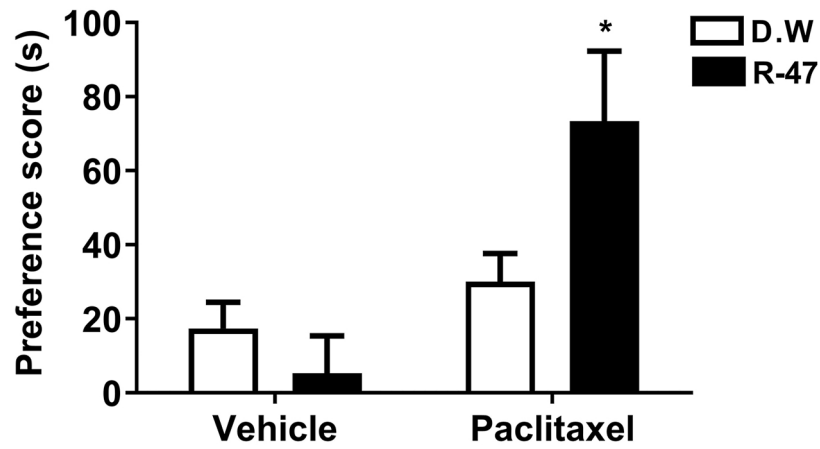
Figure 4.
R-47 induces CPP in mice with paclitaxel-induced neuropathy. A) Timeline depiction of the CPP test. B) The administration of R-47 at a dose of 10 mg/kg p.o. induces CPP in paclitaxel-treated mice, but not in vehicle-treated mice. *P < 0.05 vs D.W.-Paclitaxel. BL, Baseline (pre-conditioning day); Test represents post-conditioning drug-free preference; D.W., Distilled Water; Veh, vehicle; Pac, paclitaxel. n = 15 per group; data expressed as mean ± SEM.
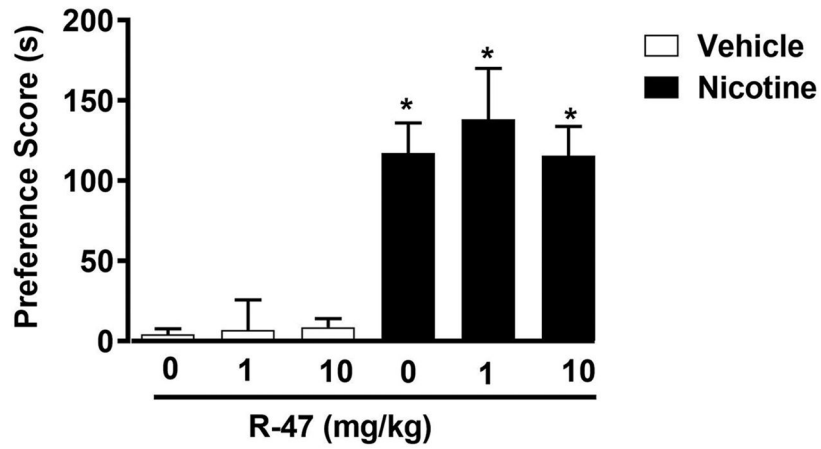
Figure 5.
Effects of R-47 on Nicotine Reward in the Conditioned Place Paradigm. Mice were conditioned with either subcutaneous (s.c.) saline or nicotine (0.5mg/kg) for 3 days. Distilled water or R-47 (1, and 10 mg/kg; p.o) pretreatment were given 120-min prior to nicotine-conditioning. Nicotine itself induces a robust place preference but R-47 pretreatment doesn't block the effect of nicotine. * Denotes $p < 0.05$ from vehicle control. Each point represents the mean ± SEM of n=10–12 mice per group.
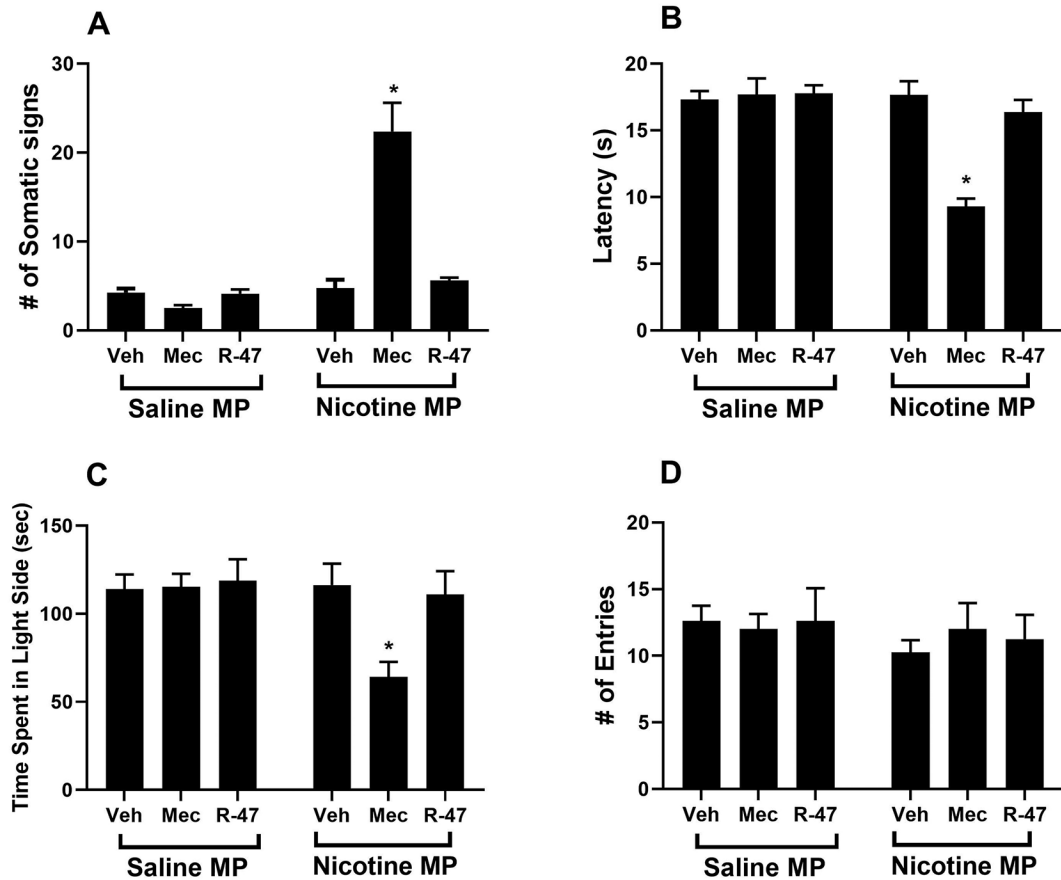
Figure 6.

R-47 Fails to Precipitate Nicotine Physical and Affective Signs. Male mice were chronically infused with saline or nicotine (24 mg/kg/day) for 14 days. On day 15, mice received subcutaneous (s.c.) injection of saline, R-47 (10 mg/kg, p.o., 120 min pretreatment) or mecamylamine (2 mg/kg; s.c., 10 min pretreatment) prior to behavioral assessment of A) somatic signs, B) hyperalgesia (hot plate latency), C) time spent in the light side (Light-Dark Box test), D) # of entries (Light-Dark Box test). Mecamylamine-Nicotine group shows withdrawal symptoms (i.e. increased # of somatic signs), but Mecamylamine-Nicotine group shows a decrease in the hot plate latency and time in the light chamber of the Light-Dark Box tests. * Denotes $p < 0.05$ vs. Saline minipump group. Each point represents the mean $\pm$ S.E.M. of n=8 mice per group. MP: minipump; Veh: vehicle; Mec: mecamylamine.
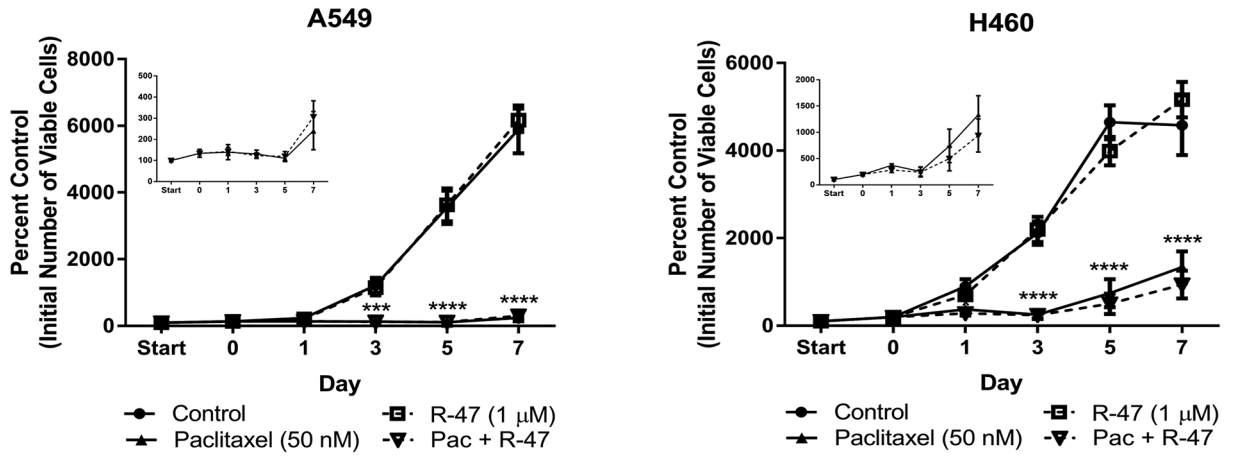
Figure 7.
R-47 does not stimulate NSCLC cell proliferation alone or interfere with paclitaxel-induced growth inhibition of NSCLC cells. The "start" time point represents the initial number of cells after seeding. A 24-hour R-47 pretreatment period occurred from Start to Day 0 for the R-47 and Pac + R-47 conditions, then all subsequent treatments lasted 24 hours; no drugs were present after Day 1. The number of viable cells was determined via trypan blue exclusion. Insets display the Pac and Pac + R-47 data on a smaller scale. ***P < 0.001, ****P < 0.0001 vs control. Data are expressed as the mean ± SEM of three independent experiments. Pac, paclitaxel.
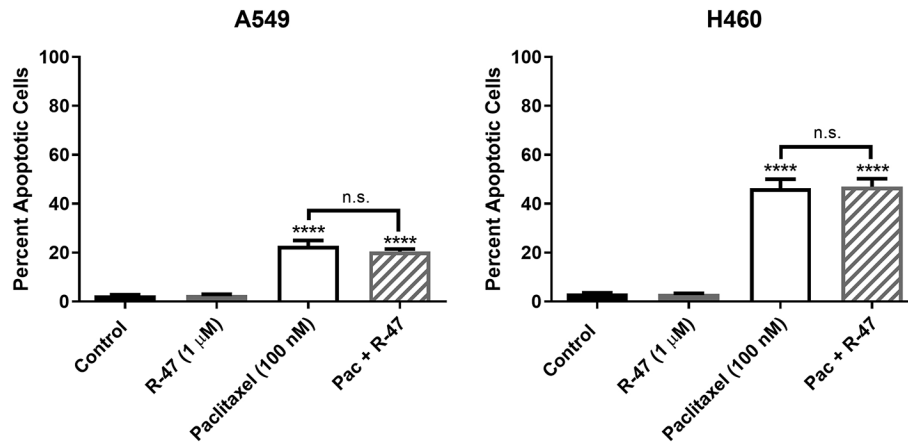
Figure 8.

R-47 does not interfere with paclitaxel-induced apoptosis of NSCLC cells. Cells were treated with R-47, paclitaxel, or the combination for 48 hours. Quantification of apoptotic cells was determined by the Annexin V/PI assay. *$P < 0.05$, **$P < 0.01$, ***$P < 0.001$, ****$P < 0.0001$ vs control; n.s., not significant ($P > 0.05$). Data are expressed as the mean ± SEM of three independent experiments. Pac, paclitaxel.
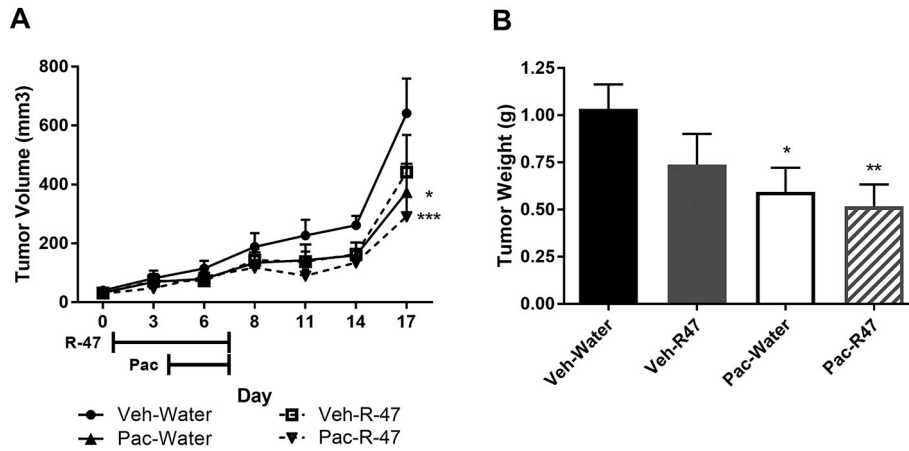
Figure 9.
R-47 does not enhance A549 NSCLC tumor growth alone or in combination with paclitaxel in NSG mice. Mice were subcutaneously injected with 1.5×10^6 cells in each flank. Once tumors became palpable, mice were given R-47 (10 mg/kg, p.o.) twice daily for 3 days starting on Day 1, then once daily in combination with paclitaxel (10 mg/kg, i.p.) for 4 days starting on Day 4. A) The left and right flank tumor volumes ($l \times w \times h$) were determined with calipers and values were averaged for each mouse. Data are expressed as mean + SEM; n = 8–9 mice per group. $*P < 0.05$, $***P < 0.001$ vs Veh-Water. B) Mice were euthanized on day 17, after which tumors were extracted and weighed; tumor weights were averaged for each mouse. $*P < 0.05$, $**P < 0.01$ vs Veh-Water. Data are expressed as mean + SEM; n = 8–9 mice per group. Veh, vehicle; Pac, paclitaxel.

Table 1.

R-47 does not interfere with paclitaxel-induced DNA fragmentation or G2/M arrest of NSCLC cells. A549 (A) and H460 (B) cells were treated with R-47, paclitaxel, or the combination for 48 hours. Cell cycle analysis was determined by propidium iodide staining and subsequent flow cytometry analysis.

A	A549				
		Phase of Cell Cycle			
	48 h Treatment	**% Sub-G1 (SEM)**	**% G0/G1 (SEM)**	**% S (SEM)**	**% G2/M (SEM)**	**% Polyploid (SEM)**
	Control	1.0 (0.3)	54.6 (5.0)	14.9 (1.6)	26.1 (1.5)	2.3 (1.3)
	R-47 1 µM	0.9 (0.2)	61.9 (1.0)[*]	12.0 (0.6)	23.4 (1.0)	1.0 (0.2)
	Paclitaxel 100 nM	19.1 (1.0)[†]	19.4 (1.0)[†]	13.8 (0.8)	35.7 (1.9)[$]	11.2 (2.3)[**]
	Paclitaxel + R47	19.9 (1.7)[†]	23.2 (1.2)[†]	14.8 (0.2)	34.7 (1.7)[**]	6.1 (0.9)
	H460				
		Phase of Cell Cycle			
	48 h Treatment	**% Sub-G1 (SEM)**	**% G0/G1 (SEM)**	**% S (SEM)**	**% G2/M (SEM)**	**% Polyploid (SEM)**
	Control	2.7 (0.8)	59.2 (0.5)	11.0 (0.1)	25.2 (0.4)	1.8 (0.3)
	R-47 1 µM	3.0 (0.3)	58.4 (0.6)	10.8 (0.2)	25.7 (0.4)	2.1 (0.3)
B	Paclitaxel 100 nM	10.1 (0.8)[†]	38.9 (1.8)[†]	12.2 (0.2)	34.8 (0.9)[†]	4.0 (0.4)
	Paclitaxel + R47	9.1 (0.4)[†]	38.0 (1.8)[†]	11.3 (0.4)	37.5 (1.5)[†]	4.2 (0.4)

[*] $P < 0.05$

[**] $P < 0.01$

[$] $P < 0.001$

[†] $P < 0.0001$ vs control.

Data are expressed as the mean of three independent experiments.

SEM, standard error of the mean.